Shape diffusion in the shell model

B. W. Bush
Theoretical Division, Los Alamos National Laboratory, Los Alamos, New Mexico 87545

G. F. Bertsch and B. A. Brown
Cyclotron Laboratory and Department of Physics, Michigan State University, East Lansing, Michigan 48824

(Received 12 September 1991)

The diffusion coefficient for quadrupolar shape changes is derived in a model based on the mixing of static Hartree-Fock configurations by the residual interaction. The model correctly predicts the width of single-particle configurations. We find a diffusion rate depending on temperature as T^3, consistent with at least one other theoretical estimate. However, our diffusion rate is an order of magnitude lower than two values extracted from data.

PACS number(s): 21.60.Cs, 21.10.Gv

I. INTRODUCTION

How fast does a highly excited nucleus change its shape? This question is important for the understanding of nuclear reactions of various kinds, including fission and the emission of statistical photons in the giant dipole region. It appears that highly excited nuclei have a hindrance in their fission decay due to the shape dynamics [1, 2]. Also, the statistical giant dipole photons should have a spectrum reflecting the range of nuclear shapes present in the ensemble, provided that shape changes take place slowly; if the changes are rapid, the width of the giant dipole is decreased by the mechanism of motional narrowing [3, 4].

Given this motivation, it is of interest to understand the theory of shape dynamics and calculate from basic interactions the parameters of the theory. Much work has been done on this subject—we can only allude to it. Among the attempts to construct a theory, there has been significant work based on linear response theory [5, 6], based on damped diabatic motion [7], and based on perturbation theory with respect to adiabatic motion [8]. In general, other workers have focused on the calculation of friction in a dynamical equation for the collective motion. A diffusion rate can then be deduced from the Einstein relation.

Our point of view here is quite different. We shall avoid completely a discussion of friction or collective motion, and concentrate exclusively on the diffusion in the nuclear shape degree of freedom. Our basic assumption—one certainly open to question—is that the highly excited nucleus can be described as an incoherent mixture of Hartree-Fock configurations at a given energy. We thus ignore single-particle motion, which can only come in indirectly through the changes in the single-particle wave functions in different Hartree-Fock configurations. The assumption of incoherence requires high excitation energy because the pairing interaction induces strong coherence between configurations near the ground state. More problematic is our assumption that self-consistent Hartree-Fock configurations exist at high excitation. We shall work in a restricted model space, the Nilsson model, where this is true, but in an unrestricted space our assumption may not be valid.

Since we assume a basis of static Hartree-Fock solutions, the dynamics comes entirely from the residual interaction. This means that only matrix elements changing the orbit of two particles simultaneously are relevant. Matrix elements between configurations with only one particle orbit changed are zero by the Hartree-Fock condition. The rate at which a state i is depopulated may be calculated from Fermi's "golden rule" if the level density is high enough. This reads

$$\Gamma = \frac{2\pi}{\hbar} \sum_f |\langle i|v_{\text{residual}}|f\rangle|^2 \, \delta(E_f - E_i) \quad , \tag{1}$$

where the sum is over Hartree-Fock states f differing by the orbital assignment of two particles. Each Hartree-Fock state has its own shape, so the shape will change by this process. We illustrate the model in Fig. 1, showing a potential energy surface in some deformation coordinate. The static Hartree solutions are shown by dots. In a constrained calculation, each dot would become a parabola, because the constraining field changes the energy and deformation of the state. The decay of the state i is illustrated by the arrows in the figure. The final states f will not differ greatly in deformation from i because only two particles have changed orbit.

This picture leads directly to a diffusion model for the shape-changing dynamics. Let us remind ourselves how the diffusion equation is derived from a discrete-basis dynamics. In Fig. 2 we show a set of discrete states, each connected to its immediate neighbors by a rate equation,

$$\frac{dP_i}{dt} = -2\Gamma P_i + \Gamma P_{i+1} + \Gamma P_{i-1}$$
$$= \Gamma \Delta_i^{(2)} P \quad .$$

The right-hand side is proportional to the second differ-

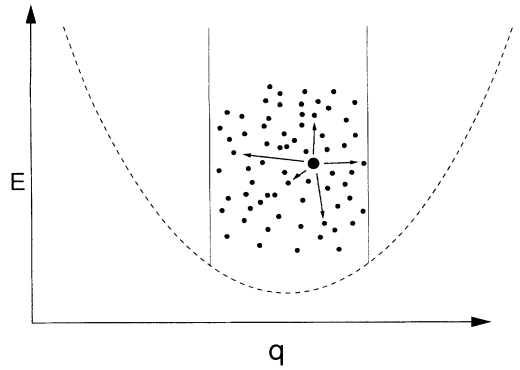

FIG. 1. Schematic view of our diffusion model. The dots represent self-consistent Hartree states, characterized by an energy E and a quadrupole moment q. The potential energy surface, indicated by the broken line, forms the lower boundary of the region containing these states. A given state, shown by the larger dot, mixes with others through the residual interaction, as indicated by the arrows. In each interaction step, the quadrupole moment changes by only a small amount.

ence operator on $P_i(t)$, as shown on the second line. If we have a continuous coordinate associated with the index i, the second difference is approximately the second derivative times the square of the step size,

$$\frac{\partial P}{\partial t} \approx \Gamma(\Delta\beta)^2 \frac{\partial^2 P}{\partial \beta^2} \quad .$$

In our situation we do not have a fixed step size, but the obviously relevant quantity is the transition rate weighted by the square of the jump in deformation. Thus our model for the diffusion will be the classical diffusion equation,

$$\frac{\partial P}{\partial t} = D_\beta \frac{\partial^2 P}{\partial \beta^2}$$

with the diffusion coefficient D_β given by

$$D_\beta = \frac{2\pi}{\hbar} \sum_f (\beta_i - \beta_f)^2 \, |\langle i|v_{\text{residual}}|f\rangle|^2 \, \delta(E_f - E_i) \quad . \tag{2}$$

The quantity $P = P(\beta, t)$ is the probability density function for the quadrupole distortion β at time t.

In the remainder of this paper we shall try to estimate D_β and find its dependence on mass number and excitation energy. We shall begin in the next section with some rough estimates. In the third section we give some results for a microscopic calculation of Eqs. (1) and (2) using a δ-function residual interaction. We then discuss other theoretical estimates, making use of the Einstein relation, and also compare with numbers extracted from experimental data.

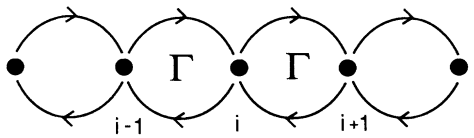

FIG. 2. Model of probability flow along a linear chain of discrete states, which leads to the diffusion equation.

II. SIMPLIFIED THEORY OF D_β

To estimate D_β from Eq. (2) we shall separately calculate the lifetime of the Hartree configurations and the mean-square change in quadrupole deformation when two particles change their orbits. We first consider the lifetime question. Empirical information is available about the lifetimes of single-particle states at moderate excitation. From particle transfer reactions we know that a state at about 8 MeV excitation has a width in the range 3–4 MeV [9]. The energy dependence of the width is predicted to be quadratic in the Fermi gas model; a phenomenological parametrization is

$$\Gamma_{\text{sp}}(E_{\text{ex}}) = \frac{{E_{\text{ex}}}^2}{20 \text{ MeV}} \quad , \tag{3}$$

where E_{ex} is the excitation energy of the state. To apply this to the multiparticle-multihole configuration representing a member of a finite-temperature ensemble, we recognize that the smearing of the Fermi surface by the finite temperature opens phase space to transitions in a way similar to the excitation energy in a simple configuration. The amount of phase available at temperature T is related to an excitation energy above a cold Fermi sphere by $E_{\text{ex}} = \pi T$ [10]. Thus, a temperature of 2.5 MeV is equivalent to an excitation energy of nearly 8 MeV, and by Eq. (3) we expect the particle to have a decay rate of about 3–4 MeV.

We have two arguments to relate the single-particle width to the decay rate of the multiparticle-multihole configuration. The first argument compares the final state phase space of the single-particle decay to that of the states in a thermal ensemble. The particle decays to two-particle–one-hole configurations whose level density is given by

$$\rho_{2\text{p}-1\text{h}} = \left(\frac{dn}{d\epsilon}\right)^3 \frac{\epsilon^2}{2} \quad ,$$

where $dn/d\epsilon$ is the single-particle level density of neutrons or protons. We assume here that the main interaction responsible for the damping is the neutron-proton interaction. The corresponding level density from a thermal ensemble may be calculated from the integral

$$\rho_{\text{thermal}} = \int dn_1 dn_2 dn_3 dn_4 \delta(\epsilon_1 + \epsilon_2 - \epsilon_3 - \epsilon_4) f_1 f_2 (1 - f_3)(1 - f_4)$$

$$\approx \left(\frac{dn}{d\epsilon}\right)^4 T^3 \int dx_1 dx_2 dx_3 dx_4 \delta(x_1 + x_2 + x_3 + x_4) f(x_1) f(x_2) f(x_3) f(x_4) \quad ,$$

where $f(x) = 1/(1+e^x)$ is the Fermi distribution function. The last integral can be evaluated exactly [11] to give

$$\rho_{\text{thermal}} = \frac{2\pi^2}{3}\left(\frac{dn}{d\epsilon}\right)^4 T^3 \quad . \tag{4}$$

Comparing the two phase spaces, we express the width of the thermal configuration as

$$\Gamma_{\text{thermal}} = \Gamma_{\text{sp}}\frac{\rho_{\text{thermal}}}{\rho_{\text{sp}}}$$

$$= \frac{4}{3}\frac{dn}{d\epsilon}T\Gamma_{\text{sp}}(E) \quad . \tag{5}$$

In accordance with the previous discussion, we assume a quadratic dependence of Γ on E and evaluate it at $E = \pi T$. For fixed energy, the single-particle width is roughly independent of A, while the density of states factor is proportional to A. Thus the A and T dependence of the width of a configuration is expected be

$$\Gamma \propto AT^3 \quad . \tag{6}$$

The identical-particle interaction will of course also contribute to the diffusion. It is in fact the pairing interaction that is mainly responsible for nuclear shape dynamics at very low excitations. However, due to the nature of the nuclear force, the identical-particle interaction should be much less important for the process we are considering. The important interaction for off-diagonal matrix elements is in the nucleon-nucleon s-wave channel. By the Pauli principle, nn or pp pairs with parallel spins cannot be in relative s states, and so the contribution from identical-particle pairs is reduced by a factor of 2. In addition, as we shall see in the next section, the strength of the identical-particle interaction is also smaller.

The second argument to relate the widths is to estimate the number of particles and holes in the thermal ensemble and to multiply the single-particle width by this factor. The average number of particles is easily determined by integrating the Fermi function over positive energies,

$$N_{\text{p}} = \int_0^\infty dn \frac{1}{e^{(\epsilon-\epsilon_F)/T}+1} \quad .$$

A similar equation applies for the number of holes. The integral is converted to one over energy which can be evaluated exactly, and we find for the total number of neutron quasiparticles

$$N_{\text{p}} + N_{\text{h}} = 2\ln 2 \frac{dn}{d\epsilon}T \quad .$$

This is multiplied by the single-particle decay rate at an excitation energy $E = \pi T$ to get the decay rate of the neutron quasiparticles. Since the protons only interact with the neutrons in this model, we do not need to consider them explicitly. The result of this estimate is practically identical to Eq. (3).

As an example, we consider the nucleus ^{76}Ge at a temperature of 2.5 MeV. Then according to Eq. (5) the single-particle width should be evaluated at $E \approx 8$ MeV. This single-particle level density is given by $dn/d\epsilon = 3A/4\epsilon_F \approx 1.8\ \text{MeV}^{-1}$, where $\epsilon_F \approx 32$ MeV is the Fermi energy. The result is

$$\Gamma_{\text{thermal}} \approx \tfrac{4}{3}(3.2\ \text{MeV})(1.8\ \text{MeV}^{-1})(2.5\ \text{MeV})$$

$$= 19\ \text{MeV} \quad .$$

Our next task is to estimate the average change in deformation that occurs when two particles jump orbits. We shall restrict ourselves to quadrupolar deformations and examine the distribution of quadrupole moments of the single-particle orbitals. If we assume no correlation between the change of orbital occupancy and the quadrupole moment, the mean-square change in the valence particle quadrupole moment is the sum of the mean-square dispersions of the single-particle moments. To estimate the dispersion in single-particle quadrupole moments, we use the harmonic oscillator model for the orbits. The mass quadrupole operator is defined

$$Q = \sum_i (2z_i^2 - x_i^2 - y_i^2) \quad ;$$

its matrix element in an oscillator state with quantum numbers (n_x, n_y, n_z) and oscillator frequency ω is given by

$$\langle Q_{\text{sp}}\rangle = \frac{\hbar}{m\omega}\sum_i (2n_{zi} - n_{xi} - n_{yi}) \quad ,$$

and the mean-square dispersion in a shell with N quanta of excitation is

$$\langle {Q_{\text{sp}}}^2\rangle = \left(\frac{\hbar}{m\omega}\right)^2 \frac{N(N+3)}{2} \quad .$$

Core polarization increases this moment by roughly a factor of 2 and the mean-square dispersion by a factor of 4. We relate this to the dispersion in deformation parameters β using the relation for near-spherical shapes,

$$\langle Q\rangle = 2\sqrt{\frac{5}{4\pi}}A\langle r^2\rangle\beta \quad .$$

Thus dispersion in β is given by

$$\langle(\beta_i - \beta_f)^2\rangle = \frac{16\pi\langle {Q_{\text{sp}}}^2\rangle}{5A^2\langle r^2\rangle^2}$$

$$\approx 6.8N(N+3)A^{-8/3} \approx 9.0A^{-2} \quad , \tag{7}$$

where we have included a factor of 4 for the number of orbitals and another factor of 4 for the core polarization enhancement. In the last part of the equation we took $\hbar\omega = 41/A^{1/3}$ and $R_0 = 1.2A^{1/3}$ fm. Multiplying this dispersion by the width, the diffusion coefficient is then given by

$$D_\beta \approx \frac{9.0\Gamma_{\text{sp}}(E)T}{A\epsilon_F} \approx \frac{170T^3}{\hbar A{\epsilon_F}^2} \quad , \tag{8}$$

with $E = \pi T$. Returning to our numerical example of ^{76}Ge, the diffusion coefficient is estimated as

$$D_\beta(A = 76, T = 2.5\ \text{MeV}) = 28\ \text{keV}/\hbar \quad . \tag{9}$$

III. MICROSCOPIC CALCULATION OF D_β

A. Nilsson model calculation

Our microscopic determination of D_β is based on the evaluation of the transition matrix element in Eq. (2) with Nilsson single-particle states and a simple δ-function residual interaction. We have used a standard single-particle Nilsson Hamiltonian [12],

$$H = -\frac{\hbar^2\nabla^2}{2m} + \frac{1}{2}m\sum_{i=1}^{3}\omega_i{}^2 x_i{}^2 - \kappa\hbar\omega_0\left[2\boldsymbol{l}\cdot\mathbf{s} + \mu\left(\boldsymbol{l}^2 - \langle\boldsymbol{l}^2\rangle_N\right)\right] \quad , \tag{10}$$

with the Hill-Wheeler parametrization [13]

$$\omega_j = \omega_0 \exp\left[-\sqrt{\frac{5}{4\pi}}\beta\cos\left(\gamma - \frac{2\pi}{3}j\right)\right] \quad ,$$

and the frequencies

$$\hbar\omega_0 = (41\ \text{MeV})A^{-1/3}\left(1 \pm \frac{1}{3}\frac{N-Z}{A}\right)$$

for protons (neutrons). Here $\langle\boldsymbol{l}^2\rangle_N$ is the expectation value of $\boldsymbol{l}^2$ in the corresponding major oscillator shell. Table I lists the values of κ and μ used in our calculation.

The Hamiltonian is diagonalized in the deformed harmonic oscillator basis $|\mathbf{n}s\rangle$, where $\mathbf{n} = (n_x, n_y, n_z)$ are the harmonic oscillator quantum numbers along the three Cartesian axes. The eigenvectors of Eq. (10) are written

$$\phi_k(\mathbf{x}) = \sum_{\mathbf{n},s}\mathcal{M}_{k,\mathbf{n}s}\psi^x_{n_x}(x)\psi^y_{n_y}(y)\psi^z_{n_z}(z)\chi_s \quad ,$$

where the ψ's are harmonic oscillator wave functions, the χ's are spinors for $j = \frac{1}{2}$, and $\mathcal{M}_{k,\mathbf{n}s} = \langle\mathbf{n}s|k\rangle$ is the diagonalizing matrix. Thus we can write the field annihilation operators as

$$a(\mathbf{x}) = \sum_k \phi_k(\mathbf{x})a_k \quad ,$$

where a_k is the annihilation operator for the orbit k.

We next calculate the matrix elements appearing in Eq. (2). The neutron-proton interaction must be treated separately from the identical-particle interaction because of the antisymmetrization. In both cases the matrix element can be written

TABLE I. Parameters for Nilsson Hamiltonian [Eq. (10)] used in the calculation.

Nucleus	Protons		Neutrons	
	κ	μ	κ	μ
^{76}Ge	0.0700	0.390	0.0730	0.290
^{110}Sn	0.0637	0.600	0.0637	0.420
^{158}Er	0.0670	0.540	0.0670	0.420

$$\begin{aligned}\langle f|v_{\text{residual}}|i\rangle &= v_c\sum_{j,j'}\langle f|\delta^{(3)}(\mathbf{x}_j - \mathbf{x}_{j'})|i\rangle \\ &= v_c\int d^3\mathbf{x}\,d^3\mathbf{x}'\langle f|a^\dagger(\mathbf{x})a^\dagger(\mathbf{x}')\delta^{(3)}(\mathbf{x}-\mathbf{x}')a(\mathbf{x}')a(\mathbf{x})|i\rangle \\ &= v_c\sum_{klmn}\langle f|a'^\dagger_k a'^\dagger_l a_m a_n|i\rangle\int d^3\mathbf{x}\,\phi'^*_k(\mathbf{x})\phi'^*_l(\mathbf{x})\phi_m(\mathbf{x})\phi_n(\mathbf{x}) \quad ,\end{aligned} \tag{11}$$

where $v_c = v_{np}, v_{nn}$ is the neutron-proton or identical-particle interaction strength. (For simplicity, we have not explicitly written the spin dependence of the residual interaction; it will be discussed shortly.) Since the initial and final states have different deformations, the self-consistent single-particle wave functions are not the same, and we distinguish with a prime the Fock operators and wave functions in the two bases. Equation (11) neglects the imperfect overlap between spectator particles. It turns out that the deformation changes are small enough so that the difference between primed and unprimed orbitals can be neglected in the above equation.

The term following the bracket in Eq. (11) is expanded as follows:

$$\begin{aligned}\int d^3\mathbf{x}\phi'^*_k(\mathbf{x})\phi'^*_l(\mathbf{x})\phi_m(\mathbf{x})\phi_n(\mathbf{x}) = \sum_{\mathbf{n}^k s^k \mathbf{n}^l s^l \mathbf{n}^m s^m \mathbf{n}^n s^n} &\mathcal{M}^*_{k,\mathbf{n}^k s^k}\mathcal{M}^*_{l,\mathbf{n}^l s^l}\mathcal{M}_{m,\mathbf{n}^m s^m}\mathcal{M}_{n,\mathbf{n}^n s^n} \\ &\times I_{n^k_x n^l_x n^m_x n^n_x} I_{n^k_y n^l_y n^m_y n^n_y} I_{n^k_z n^l_z n^m_z n^n_z} S_{s^k s^l s^m s^n} \quad ,\end{aligned}$$

where I is the integral of four harmonic oscillator wave functions (see the Appendix) [14]. The spin structure of the matrix element, contained in the factor S, depends on whether m and n (or k and l) are orbits of identical particles. We assume no spin dependence in the neutron-proton interaction, and pure singlet interaction between identical particles. Then S is given by

$$S_{s^k s^l s^m s^n} = \begin{cases}\delta_{s^k s^n}\delta_{s^l s^m} & \text{for } np \text{ configurations} \\ \frac{1}{2}(1-\delta_{s^k s^l})(1-\delta_{s^m s^n}) & \text{for } pp \text{ and } nn \text{ configurations}\end{cases}$$

We also need to calculate the change in quadrupole

moment in Eq. (2) in order to find D_β. In our basis the quadrupole moment of a single-particle orbital is

$$\langle k|Q|k\rangle = \frac{\hbar^2}{2m}\sum_{\mathbf{ns}} |\mathcal{M}_{k,\mathbf{ns}}|^2 \times \left(2\frac{2n_z+1}{\hbar\omega_z} - \frac{2n_x+1}{\hbar\omega_x} - \frac{2n_y+1}{\hbar\omega_y}\right).$$

The total quadrupole moment is just

$$q = \sum_k n_k \langle k|Q|k\rangle \quad , \tag{12}$$

where the n_k are the occupation numbers for the orbitals. The oscillator frequencies should of course be adjusted to minimize the total energy of the configuration. Instead of this, we change the oscillator frequencies to make the expectation the quadrupole part of the momentum tensor vanish: $\sum_k n_k\langle k|K_Q|k\rangle = 0$, where

$$\langle k|K_Q|k\rangle = \sum_{\mathbf{ns}} |\mathcal{M}_{k,\mathbf{ns}}|^2 [\, 2\hbar\omega_z(2n_z+1) - \hbar\omega_x(2n_x+1) - \hbar\omega_y(2n_y+1)] \tag{13}$$

and $K_Q = \hbar^2(2\nabla_z^2 - \nabla_x^2 - \nabla_y^2)/2m$. This procedure provides a core-polarization contribution to the total quadrupole moment which comes out very similar to the simple estimate of a factor of 2 increase over the valence-particle contribution.

We examine the transitions for an ensemble of initial configurations chosen from the canonical ensemble using the Metropolis method. We will also examine the behavior as a function of the energy of the initial configuration, in which case they may be regarded as representatives of the microcanonical ensemble. The δ function in Eq. (2) is represented by

$$\delta(E_f - E_i) \approx \frac{\theta(\Delta E_{\max} - |E_f - E_i|)}{2\Delta E_{\max}} \quad , \tag{14}$$

where $\theta(E)$ is the step function. This completes our discussion of the calculation of the quantities appearing in Eq. (2).

B. Determination of the interaction strength v_c

In order to find Γ and D_β we must choose the strength of the interaction, v_c, for the np and pp/nn matrix elements. The most fundamental point of view would be to take the interaction from effective Brueckner interaction based on a realistic two-nucleon potential. One could also take a more phenomenological approach and adjust the interaction to fit Γ, thus only demanding that the model predict the ratio of D_β/Γ.

Let us first discuss the more fundamental approach. The Brueckner G-matrix interaction is rather complicated, with strong spin dependence and both an attractive and a repulsive character at different momentum transfers. A reasonable average for the matrix elements we need is to weight equally all momentum-changing transitions at the Fermi surface. We shall use a G-matrix parametrized as a function of momentum transfer only, so that the average is given by the simple expression

$$\langle V\rangle = \int d\Omega\, v\left(q = 2p_f \cos\frac{\theta}{2}\cos\frac{\phi}{2}\right) \quad .$$

A G-matrix parametrization appropriate for valence particles is given in Ref. [15]; we used their Reid central interaction in our average. From the singlet-even ($T = 1$) G matrix we find $v_1 = v_{nn} = 410$ MeV fm^3, while the triplet-even ($T = 0$) yields a $v_0 = 650$ MeV fm^3 contribution to v_{np}. This implies an average np strength of 530 MeV fm^3 and a strength for the identical-particle interaction of 410 MeV fm^3.

A more phenomenological way to estimate the interaction strength is to fit nuclear structure properties. The pairing gap is very dependent on the off-diagonal interaction; in Ref. [16] a δ-function interaction was used to calculate pairing in heavy nuclei and the empirical data was fit with a strength of 340 MeV fm^3. This value is lower than the G-matrix average, which is not surprising because the average weights lower-momentum components of the interaction more heavily.

There is no equivalent property in nuclear structure that depends sensitively on the off-diagonal np interaction. The spectra of np states in odd-odd nuclei of course depends on the interaction, and these spectra have been used to extract empirical np interactions [17]. The volume integral of the np interaction in this reference has a value 900 MeV fm^3, which seems too large for our matrix elements. These interactions have long-range components which would not contribute significantly to the off-diagonal matrix elements, but which affect the total volume integral. Another study compared δ function interactions with and without a long-range monopole term to fit energy levels in the sd shell [18]. The fit with only a δ function gave $v_0 = 750$ MeV fm^3 and $v_1 = 175$ MeV fm^3, implying $v_{np} = 460$ MeV fm^3. Allowing additional monopole terms, the corresponding δ-function strengths were $v_0 = 540$ MeV fm^3, $v_1 = 390$ MeV fm^3, and $v_{np} = 460$ MeV fm^3. One final measure measure of the interaction strength is the nuclear potential. The real part of the optical model potential for low-energy neutron scattering has a volume integral per target nucleon in the range 450–500 MeV fm^3 [19].

The effective Hamiltonian is well understood for light nuclei, where essentially all of the structure can be interpreted with a Hamiltonian space that incorporates the entire major shell [20]. We can make an independent check of interaction strengths by comparing similar calculations using the empirical Hamiltonian. For this purpose we have examined the Hamiltonian for ^{20}Ne, describing four valence particles in the sd shell. We take as unperturbed states the SU(3) states in this space. These states diagonalize the quadrupole operator, and so have the maximum localization in shape. [There is one difference from the treatment with the Nilsson model, however: the SU(3) states have good angular momentum, unlike the Nilsson states.] We then calculate the mixing between the basis states using the perturbative formulas Eqs. (1) and (2) and various approximations to the Hamiltonian. The results are displayed in Table II. We first consider the effect of the δ-function interactions in this space, which are the first three entries. The first

TABLE II. Widths of SU(3) states in the nucleus ^{20}Ne, calculated from Eq. (1). The exact Hamiltonian is the W interaction from [20]. An average is taken over all SU(3) states of 4 particles in the sd shell having angular momentum $J = 2^+$. The energy of the states are expectation values of the Hamiltonian, and the δ function is represented by a normalized sum over all final states in an energy interval of width 4 MeV centered at the energy of the initial state.

Hamiltonian	v_0 (MeV fm^3)	v_1 (MeV fm^3)	Γ (MeV)
delta	0	-340	0.3
delta	-560	0	2.1
delta	-560	-340	2.8
2-body empirical			3.3
full empirical			10.6

entry shows the width due to an identical-particle interaction of strength 340 MeV fm^3 by itself, and the second entry shows the width due to the neutron-proton interaction, taken with a strength of 560 MeV fm^3. We see that the identical-particle interaction has a much smaller effect than the neutron-proton interaction, but is not entirely negligible. The third entry shows the combined effect of the two interactions. It may be seen that they are not quite additive as expected, perhaps because there are only four particles in the valence space. In the next two entries we compare the widths calculated from the matrix elements of the empirical Hamiltonian. Entry 4 shows the results using only the two-body part of the Hamiltonian. This is most comparable to desired calculation, and it may be seen that the width is fairly close to the width from the δ-function interactions. In the last entry we show the width calculated from the full empirical interaction. Here the one-particle terms in the Hamiltonian (mainly the $d_{5/2}$-$d_{3/2}$ splitting) make the widths of the pure SU(3) states very large. We shall return to this point in the conclusion.

In the remainder, we adopt as our *a priori* interaction strengths the values $v_{np} = 500$ MeV fm^3 and $v_{nn} = 340$ MeV fm^3. We are fairly confident about the identical particle interaction, but would place at least 25% uncertainty on the strength of the np interaction. In the end, the strongest basis for estimating the diffusion coefficient will be from the ratio D_β/Γ, using other estimates (or measurements) of Γ to infer D_β.

C. Numerical results for ^{24}Mg,^{76}Ge, ^{110}Sn, and ^{158}Er

In this section we examine the numerical results of the model for a range of nuclei. The lightest one we consider is the nucleus ^{24}Mg, where we can directly compare with a complete shell model calculation. However, this nucleus is really too small for statistical arguments to be valid and our main emphasis will be on the nucleus ^{76}Ge. This was chosen because the level density is high enough to justify our approximations, but the number of particle-hole configurations is small enough to permit rapid calculation. Calculations for ^{110}Sn and ^{158}Er are also presented here; they will be related to experiment in a later section.

We first test our interaction by calculating the width of a single-particle state in ^{76}Ge. Taking a state at 9.1-MeV excitation, we find a width of 3.3 MeV, in good agreement with the empirical formula.

To calculate the finite-temperature diffusion coefficient, we selected initial states from the canonical ensemble at a temperature $T = 2.5$ MeV. We required the states to have a deformation in the vicinity of $\beta = 0.16$, which is the ground-state deformation. The spectrum of ^{76}Ge in our Nilsson calculation has a level density near the Fermi level of 2.0 and 2.6 MeV^{-1} for protons and neutrons, respectively, so the average energy will be $E_{ex} \approx \pi^2 (dn_p/d\epsilon + dn_n/d\epsilon) T^2/4 \approx 70$ MeV. We calculate matrix elements to final states within an energy interval given by $\Delta E_{max} = 2$ MeV.

The average contributions to Γ and D_β from this ensemble are shown in Table III. Note that the identical-particle interaction makes only about a quarter of the total, in agreement with the argument in Sec. II. The predicted width, $\Gamma = 26.3$ MeV, is in good agreement with Eq. (4). We might have expected to underpredict the width, because there are omitted collective effects that increase the width of single-particle states [9]. It is likely that the interaction strength is somewhat high in compensation. In any case, the agreement here allows us with reasonable confidence to use the same interaction strength for the diffusion coefficient.

We now examine the distribution of widths of the states within the ensemble. Figure 3 shows the widths of the states as a function of their excitation and Fig. 4 shows the average width in the ensemble. The width obviously increases with excitation energy, but the scatter is too large to ascertain the precise dependence on E_{ex}.

TABLE III. Decay widths and diffusion coefficents for various nuclei at temperature $T = 2.5$ MeV. The interaction strengths are $v_{pp} = v_{nn} = 340$ MeV fm^3, and $v_{np} = 500$ MeV fm^3. Also included in the table are the coresponding quantities for ^{24}Mg, calculated with the empirical two-body Hamiltonian. The uncertainties in the results due to the Monte Carlo averages and sums are approximately 8%, 16%, and 42% for ^{76}Ge, ^{110}Sn, and ^{158}Er, respectively.

Nucleus	Γ (MeV)			D_β (keV)			D_β/Γ
	$(pp)+(nn)$	(np)	Total	$(pp)+(nn)$	(np)	Total	(10^{-3})
^{24}Mg			3.1			30	10.0
^{76}Ge	7.3	19.0	26.3	2.7	4.6	7.3	0.28
^{110}Sn	7.7	21.8	29.5	1.5	3.1	4.6	0.16
^{158}Er	14.9	41.6	56.5	1.3	2.6	3.8	0.067

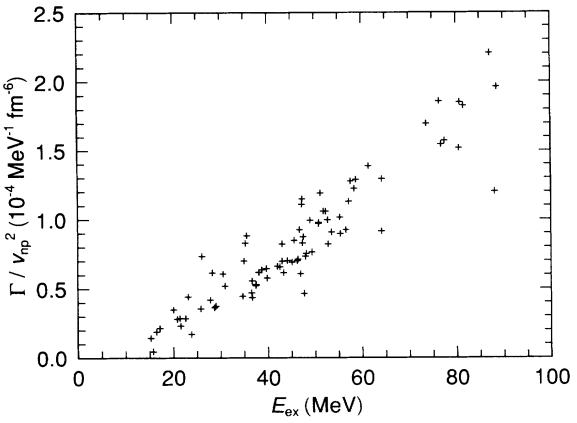

FIG. 3. Distribution of initial states contributing to the Γ of Eq. (1) for ^{76}Ge at $T = 2.5$ MeV (np configurations only).

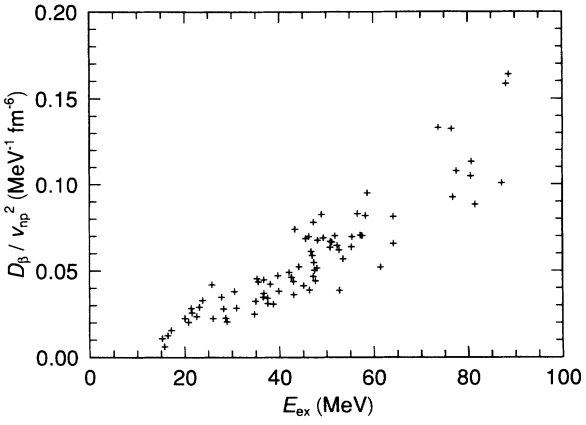

FIG. 5. Distribution of initial states contributing to the D_β of Eq. (2) for ^{76}Ge at $T = 2.5$ MeV (np configurations only).

The increase is certainly faster than linear in E_{ex}, and it is consistent with $E_{ex}{}^{3/2}$. The 3/2 power law is predicted from Eq. (6), replacing the temperature T in that equation by $\sqrt{E_{ex}}$.

Figure 3 also shows that there are substantial fluctuations in Γ at fixed E_{ex}. The configurations have an average of about 10 quasiparticles, so fluctuations of magnitude $\sqrt{1/10}$ might be anticipated. In heavier nuclei these fluctuations will be smaller and our assumption that we can treat all configurations (of fixed E_{ex}) as having the same width is reasonably justified.

In Fig. 5 we show the distribution of D_β for the same ensemble of ^{76}Ge states; Fig. 6 shows the average as a function of excitation energy. Again, D_β is fairly well defined with some fluctuation, and there is a pronounced energy dependence similar to what we found for Γ. Here also an $E_{ex}^{3/2}$ dependence is predicted, since the change in ΔQ^2 with excitation is negligible. The average value of D_β is 7.3 keV with our interaction strengths. This is smaller than the estimate in Eq. (9) by a factor of 4. This is not surprising: the orbital overlaps will be poorer when there is a large change in quadrupole moment. This produces an anticorrelation between large matrix elements and large changes in q, an effect ignored in our estimate in Sec. II.

In Figs. 7–9 we present additional statistical information about the calculation. One question is the extent to which a single term or a few terms dominates the sum in Eq. (2). The perturbative rate equation depends on there being many contributions of comparable strength. Figure 7 shows the decomposition of the relevant quantity for a typical configuration. We see that the sum in D_β arises from a multitude of weak transitions rather than a few strong ones, supporting our use of Eq. (2).

We next examine the distribution in quadrupole moment change and energy change of the transitions. This is displayed in Fig. 8. The diffusion model is only applicable if the change in q is small for each transition. This is seen to be the case; the maximum quadrupole moment change seen in the figure ($\Delta q \approx 50$ fm^2) corresponds to

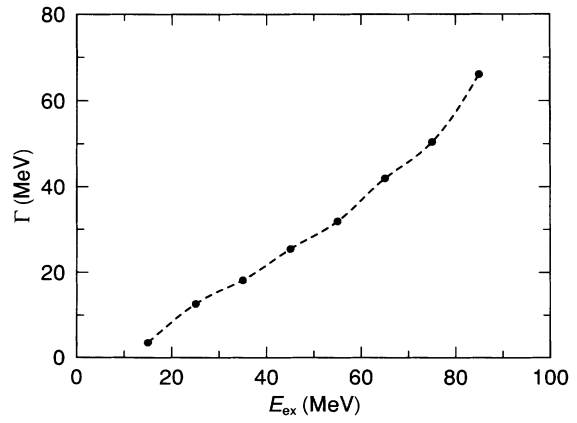

FIG. 4. Average Γ of Eq. (1) for ^{76}Ge as function of excitation energy. The solid circles are the averages and the dashed line is a smooth curve through them.

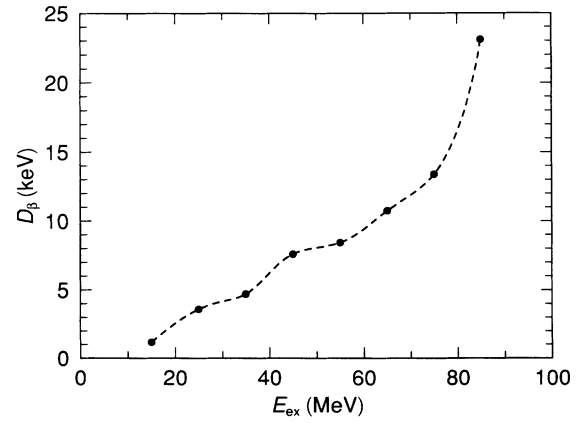

FIG. 6. Average D_β of Eq. (2) for ^{76}Ge as function of excitation energy. The solid circles are the averages and the dashed line is a smooth curve through them.

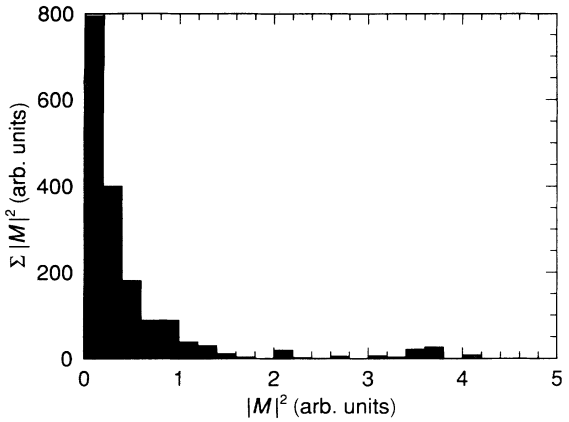

FIG. 7. Residual interaction matrix element, M, distribution for ^{76}Ge at $T = 2.5$ MeV.

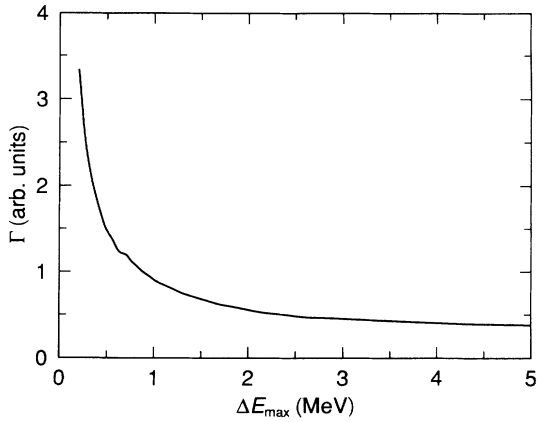

FIG. 9. Dependence of Γ on the energy cutoff $\Delta E_{\max}$ of Eq. (14) for ^{76}Ge at $T = 2.5$ MeV (*np* configurations only).

a deformation change of $\Delta\beta \approx 0.1$. The distribution in energy change should be uniform if the results are to be independent of the averaging interval $\Delta E_{\max}$. This also seems to be reasonably satisfied (see Fig. 9).

At this point we should emphasize that our Nilsson calculation is performed at a fixed deformation value. Thus when a transition that changes the quadrupole moment occurs the new state will no longer be in equilibrium at that deformation. Hence we expect the quadrupole part of the kinetic energy, K_Q of Eq. (13) to be greater for larger Δq; Fig. 10 demonstrates this clearly. In fact it is possible to find at which deformation the new configuration is in equilibrium by varying β until K_Q vanishes; we have found that the corresponding change in quadrupole moment coincides with the prediction of Eq. (12).

We next examine the dependence of Γ and D_β on the nuclear size. From Table III, we see that the width increases with mass number A. In the rough estimate Eq. (6) we predicted a linear dependence on A. Comparing ^{76}Ge and ^{158}Er, this seems to be the case, but the ^{110}Sn is anomalously low. It should be noted, however, that Sn is a semi-magic nucleus and thus would have a lower than average level density.

The diffusion coefficient D_β should decrease in heavier nuclei as A^{-1}, according to Eq. (8). From Table III we see a decreasing trend that is consistent with this behavior, recognizing that there are substantial shell fluctuations from nucleus to nucleus. The A dependence of our results can be fit with the formula

$$D_\beta \approx \frac{50T^3}{\hbar A\epsilon_f{}^2} \quad . \tag{15}$$

Finally, we present calculated values of Γ and D_β for the mixing of SU(3) states in the nucleus ^{24}Mg. Here the interaction was the two-body part of the Hamiltonian of Ref. [20], and the average was obtained from the lowest 100 states out of about 1000 total. Both the width and the diffusion constant are seen to scale from the heavier nuclei as expected. The ratio of diffusion coefficient to width has a value 0.010, to be compared with the estimate 0.015 from Eq. (7).

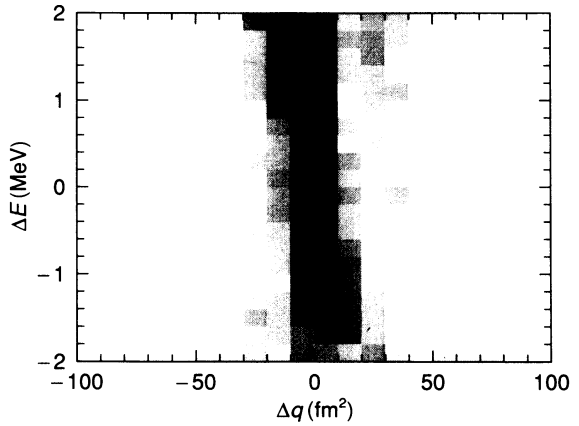

FIG. 8. Transition strength, $|M|^2$, density as a function of quadrupole moment change Δq and energy change ΔE for ^{76}Ge at $T = 2.5$ MeV.

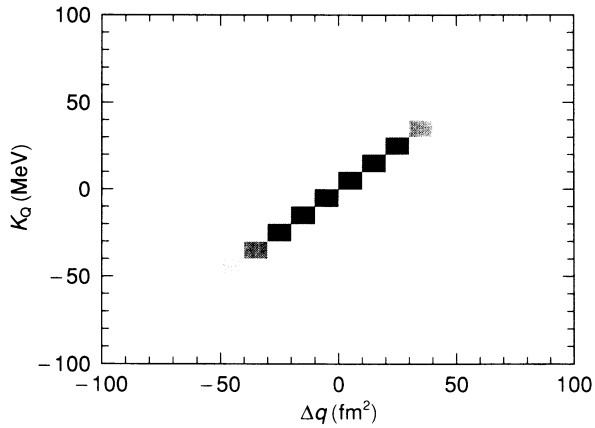

FIG. 10. Correlation between Δq and K_Q for ^{76}Ge at $T = 2.5$ MeV.

TABLE IV. Translation of collective coordinates.

Coordinate name	Ref.	Translation	Method
$\alpha_{2\mu}$	[4]	$\sum_\mu \alpha^*_{2\mu}\alpha_{2\mu} = \beta^2$	Small amplitude
γ	[7]	$\gamma = \sqrt{5/16\pi}\beta$	Small amplitude
α_2	[28]	$\alpha_2 = \sqrt{5/4\pi}\beta$	Small amplitude
z	[6]	$z = 10\beta$ fm	Distance to saddle

To summarize, we can get a rather good understanding of the diffusion model for heavy nuclei from the rough considerations of Sec. II. It is only necessary to decrease the diffusion coefficient by a factor of 3–4 to account for the correlation between matrix elements and changes in the quadrupole moment.

IV. COMPARISON WITH OTHER WORK

A. Theory

There are a number of theoretical approaches to the dynamics of large amplitude motion [4,21,22], and we wish to make the connections between the different equations of motion and compare values of the parameters. In the literature the emphasis has been on the calculation of a linear friction coefficient χ in a Newtonian equation of motion,

$$M\ddot{\alpha} + \chi\dot{\alpha} = F \quad ,$$

where α is some deformation coordinate, M is the inertial mass associated with that coordinate, and F is a generalized force. Once one has the friction coefficient χ, the diffusive dynamics can be included by adding a Langevin force to F. The resulting Langevin equation is used in Ref. [4].

An equivalent formulation is with the Fokker-Planck equation, which describes the evolution of the phase-space probability distribution for the collective coordinate. In the overdamped limit the probability distribution $P(\alpha, t)$ satisfies the Smoluchowski equation [23]

$$\frac{\partial P}{\partial t} = -\frac{\partial}{\partial \alpha}\left(-\frac{1}{\chi}FP\right) + D_\beta \frac{\partial^2 P}{\partial \alpha^2} \quad , \tag{16}$$

where

$$D_\beta = T/\chi \quad . \tag{17}$$

The last equation is the Einstein relation. The above equations can be derived from the purely diffusive dynamics discussed in the Introduction by making the rate Γ proportional to the density of final states ρ, with ρ depending on the excitation energy of the system at fixed deformation. One then obtains Eqs. (16) and (17) [24], but with T in the Einstein relation given by $T^{-1}(E,\alpha) = \rho^{-1}\partial\rho(E,\alpha)/\partial E$. Thus the Einstein relation should be applicable to the extent that T may be considered constant for all deformations of interest. For fission or other decay processes, this requires that the excitation energy be large compared to any barriers to the decay. We note that the validity of the Einstein relation in this context is discussed in Ref. [25]. They find it to be a sensible approximation in the temperature range we consider, $T \approx 2$ MeV.

TABLE V. Comparison of theoretically and experimentally extracted diffusion coefficients for ^{158}Er at 2 MeV temperature.

Source	Value
Present theory	2.0 keV
Diabatic friction [7]	2.7 keV
Linear response [6]	12.4 keV[a]
Prescission neutrons [1]	$\gtrsim$ 40 keV
Dipole narrowing [4]	50 keV[a]

[a]These numbers are scaled to $A = 158$ using Eq. (15).

Before we can compare friction coefficients in the literature, we have to translate the many different definitions of the collective coordinate to a common one. In many cases the definition reduces to a pure quadrupole distortion in the small amplitude limit, and we can make the connection in that limit. In Ref. [6] the collective coordinate has dimensions of length and we compare it to β by equating the deformation distance from a spherical shape to the fission saddle point in the two cases. For a nucleus with $A \approx 210$, this is 14 fm in the coordinates of Ref. [6] and $\beta \approx 1.4$ in quadrupole distortion. Table IV shows the translation to our variable β for the various calculations we discuss.

We now consider the model of Noerenberg [7]. He derives a formula for the friction coefficient; using the β deformation variable the formula is $\chi = 3A\epsilon_F\tau_{\rm loc}/8\pi$. Here $\tau_{\rm loc}$ is a local equilibration time which he estimates to be 0.5×10^{-22} s at $T = 2.5$ MeV. We apply this to ^{158}Er using the Einstein relation and find a diffusion coefficient in good agreement with our own calculation, as may be seen in Table V. In [26] a formula is given for $\tau_{\rm loc}$ in terms of physical quantities including an effective scattering cross section σ and nuclear matter density n_0. This combined with Noerenberg's formula yields a diffusion coefficient

$$D_\beta = \frac{68\sigma v_F n_0 T^3}{A\epsilon_F^3} \quad . \tag{18}$$

This has the same functional dependence on T and A as Eq. (15) and is numerically quite similar, if the parameters are given their usual values: $\sigma = 40$ mb, $v_F = 0.28c$, $n_0 = 0.16$ fm^{-3}.

We note that an equation similar to Eq. (2) has also been derived by Ayik [27], who started from a different point of view. Following the technique of Ref. [22], he obtains an expression which treats the nucleon interactions as scattering between particles in plane-wave states,

$$D_\beta = \left(\frac{d\beta}{dK_Q}\right)^2 \int d1d2d3d4\,(\Delta K_Q)^2\,|v|^2 f_1 f_2(1-f_1)(1-f_2)(2\pi)^4\delta(p_1+p_2-p_3-p_4)\delta(\epsilon_1+\epsilon_2-\epsilon_3-\epsilon_4) \quad .$$

Here the ϵ and p are the energies and momenta and f is the Fermi distribution function. Making a simple estimate of the collision integral, he finds a formula similar to Eq. (17).

We next compare with the numerical calculation of Ref. [6], which follows the linear response technique. The authors consider the fission of an $A = 212$ nucleus at a temperature of $T = 2$ MeV. The average friction coefficient from their Fig. 6 is about $\chi = 300\hbar$, when converted to our coordinate. The corresponding diffusion coefficient is about a factor of 2 larger than the microscopic calculation or the Noerenberg estimate, as may be seen in Table V. To make their estimate, the authors of Ref. [6] assume a single-particle damping rate somewhat smaller than in Eq. (3), so naively one would expect a lower diffusion coefficient. Perhaps, like in Eq. (8), an imperfect overlap between transitions equilibrating the shape and transitions damping the single-particle motion produces an overestimate.

B. Comparison to experiment

We first consider the experimental information on dynamic effects in fission. In Ref. [29], prescission neutron emission was analyzed to determine the magnitude of the reduced friction coefficient β_f. This is defined by $\beta_f = \eta_2/M_2$. It has units of inverse time, and from the experimental data of Ref. [1] an upper limit of 5×10^{21} s^{-1} was found. The mass parameter for the quadrupolar distortions in the α_2 coordinate of Table IV is given in Ref. [25] by $M_2 = 3mAR_0{}^2/10$, where m is the nucleon mass and R_0 is the nuclear radius. Then the friction coefficient in our units has the bound $\chi \lesssim 60\hbar$. To find the diffusion coefficient we also need the temperature. The excitation energy of the system studied, ^{158}Er, was about 180 MeV, corresponding to a temperature of about 2.5 MeV. From the Einstein relation, Eq. (17), one finds the bound on the diffusion coefficient given in Table V. It is an order of magnitude larger than our calculation.

There is also information about the friction coefficient from the energy dissipation as the fissioning nucleus moves from the saddle point to scission [30]. In Ref. [25], the extracted friction coefficient has a value $\chi = 30\hbar$ in our units, which is well within the bound obtained from the prescission neutron data. However, the diffusion time scale plays no direct role in the energy dissipation past the saddle point, and without a definite temperature it is not clear how to relate this information to the diffusion coefficient.

The analysis of the shape of the giant dipole in hot nuclei in Ref. [31] found that dynamic shape fluctuations were not required to fit the data for the nucleus for rare-earth nuclei such as ^{158}Er. From Ref. [4], this implies that the friction parameter χ is greater than about $50\hbar$. On the other hand, the data on tin nuclei favored a motional narrowing effect with $\chi \approx 30\hbar$. Here the temperature of the system was about 2 MeV, which corresponds to a diffusion coefficient

$$D_\beta(A = 110, T = 2.0 \text{ MeV}) \approx 70 \text{ keV} \quad ,$$

which is once again a factor of 10 larger than our estimate.

V. CONCLUSION

We see that our model seems to make nuclei less fluid than the available experiments indicate. We believe that our treatment of the diffusion due to two-body interactions is done well enough so that one must find another mechanism to explain the data.

In looking for a way out of this quandry, one possibility is that the dominant diffusion mechanism could occur entirely by single-particle motion, i.e., within mean-field theory ignoring the residual interaction. Note that the *sd*-shell calculation given in Table II showed that the one-body Hamiltonian produced a larger diffusion coefficient than the two-body interaction. At low excitation the mean-field configurations seem to be rather frozen, but it is not clear what would happen at higher energy when artificial symmetry constraints are dropped from the time-dependent mean-field calculations. It would be interesting to follow an ensemble of highly excited configurations within the time-dependent theory to answer this question.

We should remember also that the analyses of the experiments depended on the existence of a linear frictional dissipation. This is by no means obvious, and it has been suggested that a cubic friction force might be better justified [8]. In this case the fluctuation-dissipation theorem gives a diffusion coefficient which would increase as the square of the temperature, assuming the friction coefficient to be independent of temperature. However, it is also clear from the analyses of [6,7] that one may expect a linear friction with a quadratic temperature dependence.

It should be possible to reanalyze the fission data on prescission neutrons entirely in terms of a diffusive process, thus avoiding the uncertainties of connecting the coefficients to friction. It might be worthwhile to do this to confirm that the diffusion is indeed faster than the two-body mechanism allows.

ACKNOWLEDGMENTS

We would like to thank Y. A. Alhassid, S. Ayik, D. Cha, H. Feldmeier, and J. R. Nix for useful discussions. This work was supported by the National Science Foundation under Grant No. 90–17077 and by the U. S. Department of Energy.

APPENDIX: N-BODY HARMONIC OSCILLATOR MATRIX ELEMENTS

We want to calculate the integral of N harmonic oscillator wave functions:

$$I = \int_{-\infty}^{\infty} dx \prod_{i=1}^{N} \psi_i(x) \quad ,$$

where

$$\psi_i(x) = \pi^{-1/4}\sqrt{\frac{b_i}{2^{n_i}n_i!}}H_{n_i}(b_i x)e^{-b_i^2x^2/2} \quad ,$$

the H_n are Hermite polynomials, and the b are the oscillator lengths. These integrals are of interest because we are using a harmonic oscillator basis for the Nilsson calculation and our residual interaction is a two-body δ function. We use the fact that the Hermite polynomials can be expressed in terms of a generating function [32]:

$$\exp(2\xi z - z^2) = \sum_{n=0}^{\infty}\frac{z^n}{n!}H_n(\xi) \quad ,$$

so that I is the coefficient of $\prod_{i=1}^{N} z_i^{n_i}/n_i!$ in

$$J = \int dx \sum_{\{n_i\}}\prod_{i=1}^{N}\psi_i(x)\frac{z_i^{n_i}}{n_i!} = \pi^{-N/4}\sqrt{\frac{\pi}{B}}\prod_i\sqrt{\frac{b_i}{2^{n_i}n_i!}}\exp\left[\frac{1}{B}\left(\sum_i b_i z_i\right)^2 - \sum_i z_i^2\right] \quad ,$$

where $B = \frac{1}{2}\sum_i b_i^2$. We can expand the exponential in terms of the z_i

$$J = \pi^{-N/4}\sqrt{\frac{\pi}{B}}\prod_i\sqrt{\frac{b_i}{2^{n_i}n_i!}}\sum_k\sum_\ell\frac{1}{k!}\frac{1}{\ell!}\frac{(-1)^\ell}{B^k}\sum_{\{\alpha_i,\beta_i\}}\binom{2k}{\alpha_1\cdots\alpha_N}\binom{\ell}{\beta_1\cdots\beta_N}\prod_i b_i^{\alpha_i}z_i^{\alpha_i+2\beta_i}$$

to identify

$$I = \pi^{-N/4}\sqrt{\frac{\pi}{B}}\prod_i\sqrt{\frac{n_i!b_i}{2^{n_i}}}\sum_{\{\alpha_i,\beta_i\}}\frac{1}{k!}\frac{1}{\ell!}\frac{(-1)^\ell}{B^k}\binom{2k}{\alpha_1\cdots\alpha_N}\binom{\ell}{\beta_1\cdots\beta_N} \quad ,$$

such that $\alpha_i + 2\beta_i = n_i$, $2k = \sum_i \alpha_i$, and $\ell = \sum_i \beta_i$. (The large parentheses are multinomial coefficients.) Note that the only selection rule that holds for $N > 2$ is that $\sum_i n_i$ be even (i.e., parity is conserved).

[1] A. Gavron *et al.*, Phys. Rev. C **35**, 579 (1987).
[2] R. Butsch *et al.*, Phys. Rev. C **41**, 1530 (1990); M. Thoennessen *et al.*, Phys. Rev. Lett. **59**, 2860 (1987).
[3] R. Broglia *et al.*, Phys. Rev. Lett. **53**, 326 (1987).
[4] Y. Alhassid and B. Bush, Nucl. Phys. **A514**, 434 (1990).
[5] H. Hofmann and P. Siemens, Nucl. Phys. **A257**, 165 (1976).
[6] S. Yamaji, H. Hofmann, and R. Samhammer, Nucl. Phys. **A475** 487 (1988).
[7] W. Noerenberg, Phys. Lett. **104B** 107 (1981).
[8] M. C. Nemes and H. A. Weidenmüller, Phys. Rev. C **24**, 450 (1981); M. C. Nemes and H. A. Weidenmüller, Phys. Rev. C **24**, 944 (1981).
[9] G. Bertsch, P. Bortignon, and R. Broglia, Rev. Mod. Phys. **55**, 287 (1983).
[10] P. Morel and P. Nozieres, Phys. Rev. **126**, 1909 (1962).
[11] G. Baym and C. Pethick, in *Physics of Liquid and Solid Helium*, edited by K. H. Bennemann and J. B. Ketterson, (Wiley, New York, 1978), Vol. 2, p. 115.
[12] G. Anderson *et al.*, Nucl. Phys. **A268**, 205 (1976); A. V. Ignatyuk *et al.*, *ibid.* **A346**, 191 (1977); K. Neergard *et al.*, *ibid.* **A287**, 48 (1977); A. V. Ignatyuk *et al.*, Nucl. Phys. **A443**, 415 (1980).
[13] D. L. Hill and J. A. Wheeler, Phys. Rev. **89**, 1102 (1953).
[14] From a numerical point of view, it is more efficient to evaluate the integral over the oscillator functions in two steps, calculating first the density and then taking the overlap of two densities.
[15] G. Bertsch *et al.*, Nucl. Phys. **A284**, 399 (1977).
[16] D. Glas and U. Mosel, Nucl. Phys. **A216**, 563 (1973).
[17] J. Schiffer and W. True, Rev. Mod. Phys. **48**, 191 (1976).
[18] B. A. Brown *et al.*, Ann. Phys. **182**, 191 (1988).
[19] J. Rapaport, Phys. Rep. C **87**, 25 (1982).
[20] B. A. Brown and B. H. Wildenthal, Annu. Rev. Nucl. Part. Sci. **38**, 29 (1988).
[21] P. Grange, L. Jun-Qing, and H. Weidenmueller, Phys. Rev. C **27**, 2063 (1983).
[22] S. Ayik *et al.*, Z. Phys. A **337**, 413 (1990).
[23] S. Chandrasekhar, Rev. Mod. Phys. **15**, 1 (1943).
[24] D. Cha (unpublished).
[25] H. Hofmann, R. Samhammer, and G. Ockenfuss, Nucl. Phys. **A496**, 269 (1989).
[26] G. Bertsch, Z. Phys. A **289**, 103 (1978).
[27] S. Ayik, private communciation.
[28] A. J. Sierk, S. E. Koonin, and J. R. Nix, Phys. Rev. C **17**, 646 (1978).
[29] P. Grange *et al.*, Phys. Rev. C **34**, 209 (1986).
[30] K. Davies *et al.*, Phys. Rev. C **16**, 1890 (1977).
[31] Y. Alhassid and B. Bush, Nucl. Phys. **A509**, 461 (1990).
[32] M. Abramowitz and I. A. Stegun, *Handbook of Mathematical Functions* (Dover, New York, 1972).

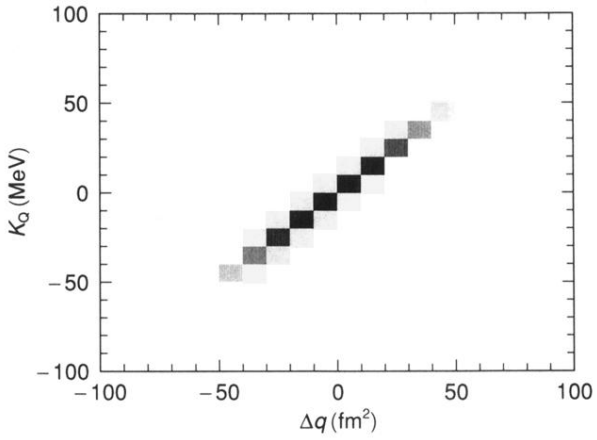

FIG. 10. Correlation between Δq and K_Q for ^{76}Ge at $T = 2.5$ MeV.

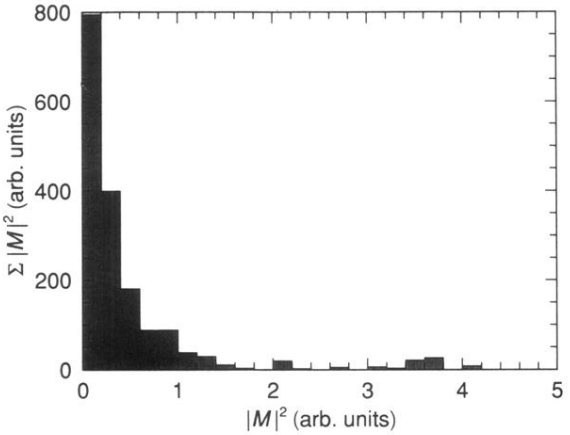

FIG. 7. Residual interaction matrix element, M, distribution for ^{76}Ge at $T = 2.5$ MeV.

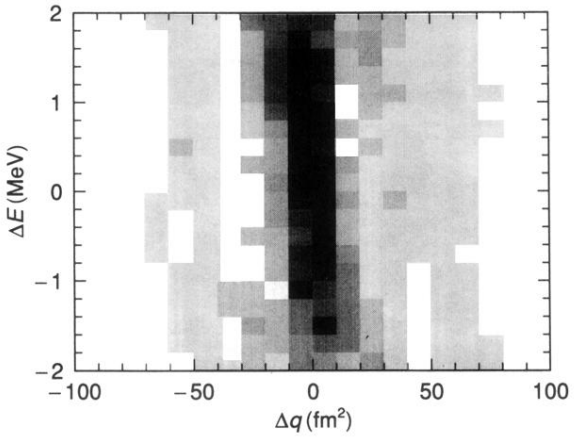

FIG. 8. Transition strength, $|M|^2$, density as a function of quadrupole moment change Δq and energy change ΔE for ^{76}Ge at $T = 2.5$ MeV.